



# Quantifying two-way influences between the Arctic and mid-latitudes through regionally increased CO<sub>2</sub> concentrations in coupled climate simulations

Tido Semmler<sup>1</sup> · Felix Pithan<sup>1</sup> · Thomas Jung<sup>1</sup>

Received: 25 February 2019 / Accepted: 5 February 2020 / Published online: 12 February 2020  
© The Author(s) 2020

## Abstract

In which direction is the influence larger: from the Arctic to the mid-latitudes or vice versa? To answer this question, CO<sub>2</sub> concentrations have been regionally increased in different latitudinal belts, namely in the Arctic, in the northern mid-latitudes, everywhere outside of the Arctic and globally, in a series of 150 year coupled model experiments with the AWI Climate Model. This method is applied to allow a decomposition of the response to increasing CO<sub>2</sub> concentrations in different regions. It turns out that CO<sub>2</sub> increase applied in the Arctic only is very efficient in heating the Arctic and that the energy largely remains in the Arctic. In the first 30 years after switching on the CO<sub>2</sub> forcing some robust atmospheric circulation changes, which are associated with the surface temperature anomalies including local cooling of up to 1 °C in parts of North America, are simulated. The synoptic activity is decreased in the mid-latitudes. Further into the simulation, surface temperature and atmospheric circulation anomalies become less robust. When quadrupling the CO<sub>2</sub> concentration south of 60° N, the March Arctic sea ice volume is reduced by about two thirds in the 150 years of simulation time. When quadrupling the CO<sub>2</sub> concentration between 30 and 60° N, the March Arctic sea ice volume is reduced by around one third, the same amount as if quadrupling CO<sub>2</sub> north of 60° N. Both atmospheric and oceanic northward energy transport across 60° N are enhanced by up to 0.1 PW and 0.03 PW, respectively, and winter synoptic activity is increased over the Greenland, Norwegian, Iceland (GIN) seas. To a lesser extent the same happens when the CO<sub>2</sub> concentration between 30 and 60° N is only increased to 1.65 times the reference value in order to consider the different size of the forcing areas. The increased northward energy transport, leads to Arctic sea ice reduction, and consequently Arctic amplification is present without Arctic CO<sub>2</sub> forcing in all seasons but summer, independent of where the forcing is applied south of 60° N. South of the forcing area, both in the Arctic and northern mid-latitude forcing simulations, the warming is generally limited to less than 0.5 °C. In contrast, north of the forcing area in the northern mid-latitude forcing experiments, the warming amounts to generally more than 1 °C close to the surface, except for summer. This is a strong indication that the influence of warming outside of the Arctic on the Arctic is substantial, while forcing applied only in the Arctic mainly materializes in a warming Arctic, with relatively small implications for non-Arctic regions.

**Keywords** Arctic amplification · Arctic mid-latitude linkages · Regional greenhouse gas forcing · Energy transport · Coupled climate model simulations

## 1 Introduction

Over the last 30 years, Arctic amplification, an increase of Arctic surface temperatures twice the amount of the Northern hemisphere mean temperature increase, has been observed in the field and in climate projections (Cohen et al. 2014). This is associated with a marked sea ice decline in the Arctic which has spurred a multitude of studies investigating the impact of this strong decline on the mid-latitude weather and climate including extreme events both from

---

✉ Tido Semmler  
tido.semmler@awi.de

<sup>1</sup> Alfred-Wegener-Institut, Helmholtz-Zentrum für Polar- Und Meeresforschung, Am Handelshafen 12, 27570 Bremerhaven, Germany

observations and modelling experiments (review papers: Overland et al. 2015; Screen et al. 2018; Vavrus 2018). In many of the modelling studies the impact of Arctic sea ice decline is mostly restricted to the stable Arctic boundary layer with only minor temperature increases higher up in the troposphere (e.g. Semmler et al. 2016a, b). Furthermore, the impact of shrinking sea ice in the Arctic on mid-latitudes remain subject to a large uncertainty due to a notoriously small signal-to-noise ratio in the northern mid-latitudes, a limited time period of observations, and different designs of modelling studies (Cohen et al. 2018). Since the specific region of sea ice loss plays a role in determining the large-scale circulation response (e.g. Pedersen et al. 2016), differences in the prescribed forcing in the idealized modelling studies can be important.

Nevertheless, progress has been made. Since feedbacks between the different climate system components such as ocean, sea ice, land, and atmosphere have been recognized to be important, a number of coupled modelling studies with long integrations of 100 years or more are available now. Screen et al. (2018) give a synthesis of long coupled model experiments which reveal some consistent features as response to sea ice loss despite differences in the model set-up: hemisphere-wide atmospheric warming, intensification of Aleutian low and Siberian high, weakening of the Icelandic low, weakening and southward shift of the mid-latitude westerly winds in winter. Semmler et al. (2016b) and Petrie et al. (2015) took a different approach, running large ensembles of short integrations of only one year rather than small ensembles of long integrations, perturbing sea ice thickness in spring or early summer. Possibly due to a different start date (1st of June versus 1st of April) and different intensities of the forcing (summer ice-free conditions versus 2007/2012 conditions), results in terms of large-scale circulation response are not consistent although a southward shift of the mid-latitude westerly winds in late autumn or early winter occurs in both studies. Due to the long ocean response time, it cannot be expected that the lower latitude ocean substantially warms in these short coupled simulations. Very recently, the response to sea ice loss has been isolated from the complete greenhouse gas impact in the coordinated multi-model ensemble of CMIP5 models (Zappa et al. 2018)—the robust results being a southward shift of the jet stream and a strengthening of the Siberian High in late winter consistent with many studies prescribing idealized sea ice conditions.

The US CLIVAR white paper by Cohen et al. (2018) has expressed a need for a common protocol for coordinated experiments to overcome the issue of different model experiment design and to further narrow down some of the uncertainties. The resulting common protocol, the Polar Amplification Model Intercomparison Project (PAMIP: Smith et al. 2018) has been endorsed by CMIP6. Experiments

within PAMIP include applying Arctic sea ice anomalies with and without SST anomalies in uncoupled and coupled mode in short 1-year and long 100-year simulations. While it was relatively straightforward to agree on a protocol for the uncoupled experiments, prescribing sea ice and SST, the design of the coupled experiments has been much more controversial since the sea ice is an interactive component of the coupled model system and thus cannot be prescribed. Therefore, the sea ice relaxation approach is only suggested in the PAMIP protocol for the coupled experiments but is not the only choice allowed to achieve a sea ice reduction (Smith et al. 2018). This motivated us to experiment with an alternative approach.

It is acknowledged that Arctic amplification is influenced not only by local processes (e.g. Pithan and Mauritsen 2014) but also by the mid- and lower latitudes such as mid-latitude SST (e.g. Luo et al. 2018) and circulation changes (e.g. Gong et al. 2017) leading to more frequent moisture intrusions into the Arctic (e.g. Woods and Caballero 2016). Many recent studies have focused on Arctic-to-mid-latitude influences. Here we ask what direction exhibits the stronger coupling: from the Arctic to the Northern mid-latitudes or vice versa. To answer this question, it is not sufficient to alter sea ice conditions as this can only be done in the polar regions, not in the mid-latitudes. Furthermore, the ocean should be included as it can play an important role in the energy transport. Therefore, long integrations are needed. To keep the computational burden manageable, we opted to run the simulations in a relatively coarse resolution. Our idea is to increase CO<sub>2</sub> forcing regionally in the Arctic and in this way trigger Arctic amplification. Results can be contrasted against simulations with CO<sub>2</sub> forcing outside of the Arctic. This approach has very recently been applied by Stuecker et al. (2018) using the Community Earth System Model CESM 1.2. We complement their study using another CMIP6 model (AWI-CM 1.1) and additionally investigate the large-scale circulation response. Furthermore, we ran the coupled system for 150 years rather than 60 years which allows us to compare the transient response in the first decades after regionally increasing CO<sub>2</sub> to the response after the ocean had time to react.

In Sect. 2 the experiment set up is described. Section 3 explains our results; discussion and conclusions follow in Sect. 4.

## 2 Experiment setup

As stated in the introduction, there is a lot of discussion about how to study the influence of declining sea ice on mid-latitudes in coupled simulations. The most common methods are applying a ghost longwave radiation forcing over the sea ice covered area, a change of the sea ice albedo,

and a relaxation of the sea ice concentration to some desired distribution such as projected end-of-the-century conditions (e.g. Screen et al. 2018). Here, we experiment with an approach to perturbing coupled models very recently introduced by Stuecker et al. (2018). The idea is to increase the CO<sub>2</sub> concentration in some area of interest. In our study, we quadruple CO<sub>2</sub> north of 60° N (experiment called 60 N hereafter), north of 70° N (70 N), north of the simulated ice edge on the 1st of January each year (SICE), in a latitude band from 30 to 60° N (30–60 N), south of 60° N (60 Ns) or globally (glob)—for an overview see Fig. 1 showing Arctic sea ice volume from the different experiments. The experiment 30° N to 60° N is additionally run with 1.65 × CO<sub>2</sub> (30–60 N\_1.65) to account for the different size of the forcing area in order to make the 30–60 N\_1.65 and the 60 N experiments directly comparable. Indeed the 30–60 N\_1.65 and the 60 N experiment have the same globally averaged radiative forcing within the error estimates. This has been checked with a Gregory diagnosis (Gregory et al. 2004):  $0.45 \pm 0.09 \text{ W/m}^2$  for the 30–60 N\_1.65 experiment and  $0.48 \pm 0.09 \text{ W/m}^2$  for the 60 N experiment.

The simulations are set up in the spirit of the HighResMIP protocol (Haarsma et al. 2016), i.e. the control simulation (ctl) is run for a total of 200 years with the first 50 years regarded as spin-up. After the spin-up period, the described sensitivity experiments are run for 150 years which are then compared to the corresponding years of the ctl simulation. All simulations are run with the Alfred Wegener Institute Climate Model version 1.1 (AWI-CM 1.1). AWI-CM has

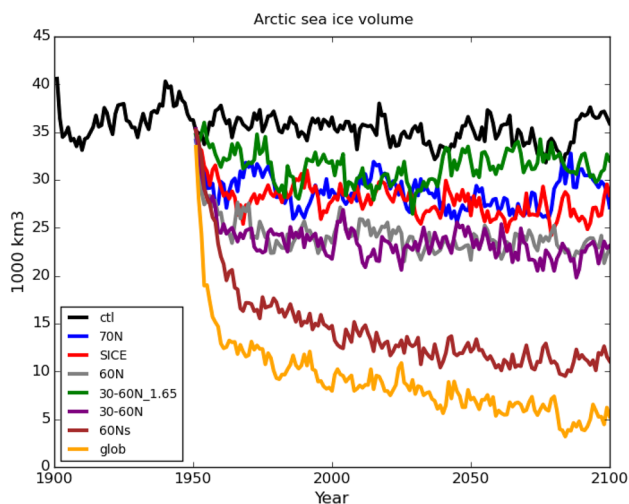


**Fig. 1** Time series of Arctic sea ice volume in March for the control integration with 1950 CO<sub>2</sub> forcing (ctl) and different sensitivity experiments, in which CO<sub>2</sub> is instantaneously increased in 1950: quadrupled north of 70° N (70 N), quadrupled north of the sea ice edge on the 1st of January each year (SICE), quadrupled north of 60° N (60 N), multiplied by 1.65 between 30 and 60° N (30–60 N\_1.65), quadrupled between 30 and 60° N (30–60 N), quadrupled south of 60° N (60 Ns), and quadrupled globally (glob)

been described in Sidorenko et al. (2015), Rackow et al. (2018, 2019). The model was run in its low resolution CMIP6 set-up (LR). The atmosphere model is ECHAM6.3 in T63L47 resolution corresponding to about 200 km horizontal resolution and 47 unequally spaced vertical levels up to 80 km. The ocean model is the Finite Element Sea ice Ocean Model FESOM 1.4 which runs on an unstructured mesh with an average horizontal resolution of around 70 km and local refinement in the tropics, the northern North Atlantic, the Arctic, and the coasts. In the vertical there are 46 unequally spaced z-levels.

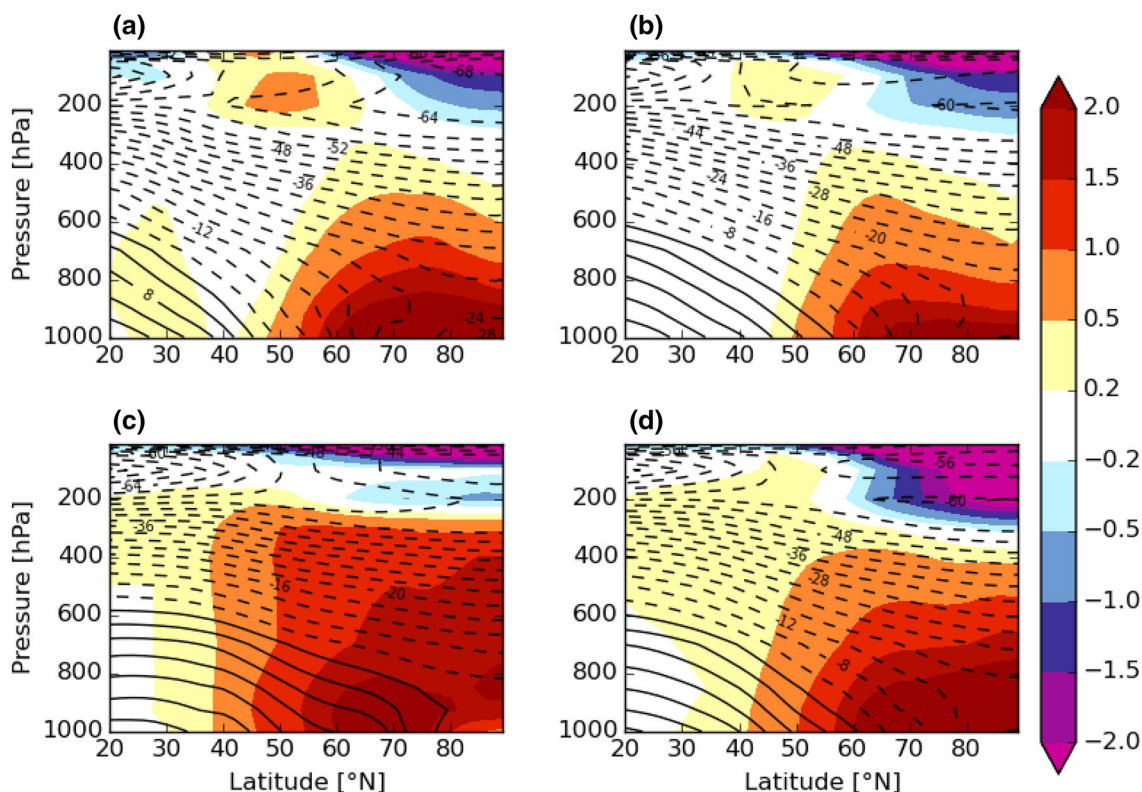
The regional CO<sub>2</sub> method has certain advantages over previously used methods, i.e. the model itself is not altered through the introduction of extra fluxes or relaxation terms which would make the model non-energy- and non-mass-conserving. Unlike the albedo reduction method, the forcing is applied all year rather than only in summer. Furthermore, it is possible to perform comparative experiments with forcing in other latitudes. However, also with this method of regionally increasing the CO<sub>2</sub> concentration the baroclinicity is altered by definition.

Figure 1 shows that the regional CO<sub>2</sub> method works to reduce Arctic sea ice quite fast within about one decade. In addition to the rapid response of the sea ice in all sensitivity experiments, a slow long-term drift possibly due to oceanic processes occurs for the global and nearly global forcing experiments (glob and 60 Ns). Even without any Arctic forcing in the 60 Ns experiment, the amount of Arctic sea ice declines markedly due to energy transport from the low to the high latitudes. If forcing is applied only in the northern mid-latitudes (30–60 N\_1.65 and 30–60 N), Arctic sea ice is also shrinking, especially in the 30–60 N experiment where the reduction is comparable to the 60 N experiment. The experiments allow study of the transient phase of rapid sea ice loss and the stabilization phase. Results regarding atmospheric temperature response, large-scale circulation, synoptic activity, and energy transport are described in the next section.

## 3 Results

### 3.1 Atmospheric temperature response

The zonally averaged vertical temperature profile anomalies for the 60 N simulation for the first 30 years after regionally quadrupling CO<sub>2</sub> are shown in Fig. 2. The profiles indicate mainly near-surface warming, except for summer where the atmospheric boundary layer is less stable and more mixing takes place. In boreal winter (DJF), noticeable warming of more than 0.5 °C is restricted to layers below 500 hPa. Laterally such warming spreads to around 48° N. In the following 120 years, the picture does not look very different (Fig. 3),



**Fig. 2** Response in zonally averaged temperature averaged over the first 30 years after quadrupling  $\text{CO}_2$  north of  $60^\circ\text{N}$  (in the Arctic) in **a** DJF, **b** MAM, **c** JJA, and **d** SON. Solid and dashed lines indi-

cate above- and sub-zero temperatures in the 1950 control simulation, shaded contours indicate anomalies in the sensitivity simulation

although the warming spreads out a little bit more laterally due to the gradual heat uptake of the ocean. Warming of more than  $0.5^\circ\text{C}$  occurs up to  $44^\circ\text{N}$  in these 120 years. In addition, slight warming of  $0.2\text{--}0.5^\circ\text{C}$  occurs almost everywhere in the troposphere north of  $20^\circ\text{N}$  which is not the case for the first 30 years. Due to the weaker forcing in 70 N and SICE simulations, warming areas are vertically more restricted in those simulations (not shown). The vertical restriction of the warming is in line with previous studies of the effects of declining sea ice (e.g. Screen et al. 2013; Semmler et al. 2016a).

In the simulations we see some stratospheric cooling (Figs. 2, 3) which is opposite from what we have observed in recent decades. This cooling becomes even stronger in the last 120 years compared to the first 30 years of the simulation. Previous simulations have shown strong intrinsic variability and inter-model differences in the stratospheric response to sea ice reduction in both uncoupled and coupled simulations (Screen et al. 2013, 2018) which could suggest that also the stratospheric warming that we have observed over the last three decades might not be due to sea ice decline but simply an expression of intrinsic variability or lower latitude impacts. Indeed, Seviour (2017) and Garfinkel et al. (2017) confirm by evaluating large ensembles

of coupled climate model simulations that vortex trends of similar magnitude to those observed can be generated by internal variability. Due to the stratospheric cooling our simulated large-scale circulation response to AA might be different compared to studies with stratospheric winter warming. It should be noted that it is not clear in which direction the stratospheric polar vortex is headed under global warming scenarios (Ayarzagüena et al. 2018).

Figures 4 and 5 show the zonally averaged vertical temperature profile anomalies for the  $30\text{--}60^\circ\text{N}$  and  $30\text{--}60^\circ\text{N}_{1.65}$  experiments. To account for the different strength of the globally averaged radiative forcing in the  $30\text{--}60^\circ\text{N}$  simulation compared to  $60^\circ\text{N}$  and  $30\text{--}60^\circ\text{N}_{1.65}$  simulations, the response in the  $30\text{--}60^\circ\text{N}$  simulation is scaled by the different forcing area between  $60^\circ\text{N}$  and  $30\text{--}60^\circ\text{N}$  simulations. As expected, the warming spreads out higher up into the troposphere in  $30\text{--}60^\circ\text{N}$  and  $30\text{--}60^\circ\text{N}_{1.65}$  experiments compared to  $60^\circ\text{N}$  experiment, generally up to  $200\text{--}300\text{ hPa}$  rather than  $500\text{ hPa}$ . Laterally, the warming mainly spreads out to the Arctic in the  $30\text{--}60^\circ\text{N}$  and  $30\text{--}60^\circ\text{N}_{1.65}$  experiments and amounts to more than  $1^\circ\text{C}$  in large areas in all seasons but summer. In contrast, south of the forcing area, i.e. south of  $30^\circ\text{N}$  the warming only exceeds  $0.5^\circ\text{C}$  in a  $2^\circ\text{--}7^\circ$  latitude belt depending on the

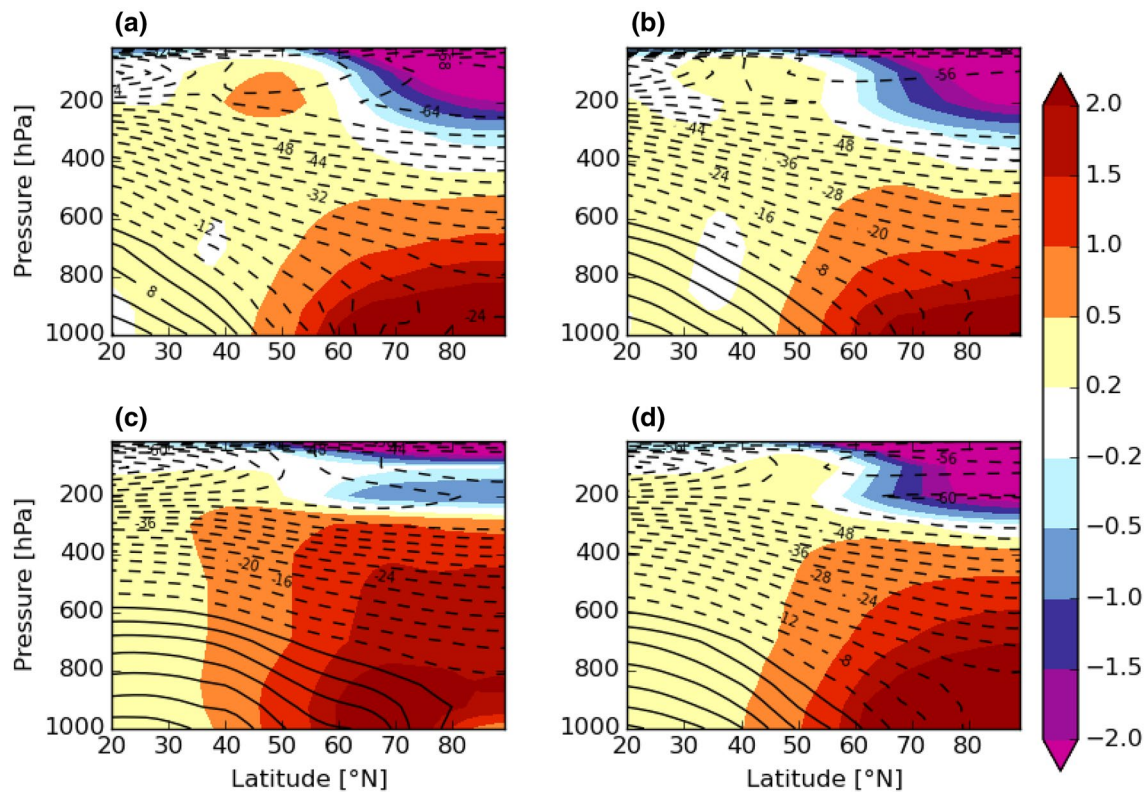


**Fig. 3** As in Fig. 2 but averaged over the last 120 years

season and on the experiment. It is reassuring that the stronger globally averaged radiative forcing in the 30–60 N simulation compared to the 30–60 N<sub>1.65</sub> simulation does not qualitatively change the vertical profile of the zonally averaged temperature response. However, even the scaled warming appears to be slightly larger in the 30–60 N simulation compared to the 30–60 N<sub>1.65</sub> simulation. In the 60 Ns experiment (Fig. 6), a largely homogeneous warming corresponding to a scaled value of 0.2–0.5 °C is simulated. Only in the subtropical troposphere as well as close to the surface in the Arctic in boreal winter (DJF), spring (MAM), and autumn (SON) larger temperature increases are simulated which resembles a typical response pattern to global CO<sub>2</sub> forcing.

Very little of the extra energy due to the regional CO<sub>2</sub> forcing spreads towards the equator; the bulk of the extra energy spreads towards the pole leading to Arctic Amplification associated with Arctic sea ice melt in all seasons but summer. The typical bottom heavy Arctic Amplification signature can be seen both in the northern mid-latitude forcing experiments (Figs. 4, 5) and in the extra-Arctic forcing experiment 60 Ns (Fig. 6). In Sect. 3.3 the meridional atmospheric and oceanic energy transport is analyzed to understand these responses.

### 3.2 Near-surface temperature response in the Arctic forcing experiments

After quadrupling CO<sub>2</sub> in the Arctic we already see strong surface warming in this region in the first 30 years—as expected (Fig. 7). In this Figure we only show changes in the 60 N experiment but the changes are consistent in the 3 experiments 60 N, 70 N, and SICE and are robust. Especially robust is the Barents Sea warming of more than 7 °C compared to the 1950 control experiment. This warming is caused by the maximum of sea ice loss in this area (not shown). In cases of northerly flows we would expect mid-latitude warming and less temperature variability due to the advection of less cold air (Semmler et al. 2012; Ayrzagüena and Screen 2016) which we indeed see in many areas, especially over central Eurasia and the North Pacific (only mean signal shown, not variability). However, we see robust boreal winter cooling by up to around 1 °C over Central North America as well as by more than 0.2 °C over eastern Asia and off its coast in the transient phase of the first 30 years after quadrupling CO<sub>2</sub> (Fig. 7a). In addition, no warming or a slight cooling of up to around 0.2 °C is simulated over the British Isles, parts of the North Atlantic and western Scandinavia, for western Scandinavia only for 70 N and

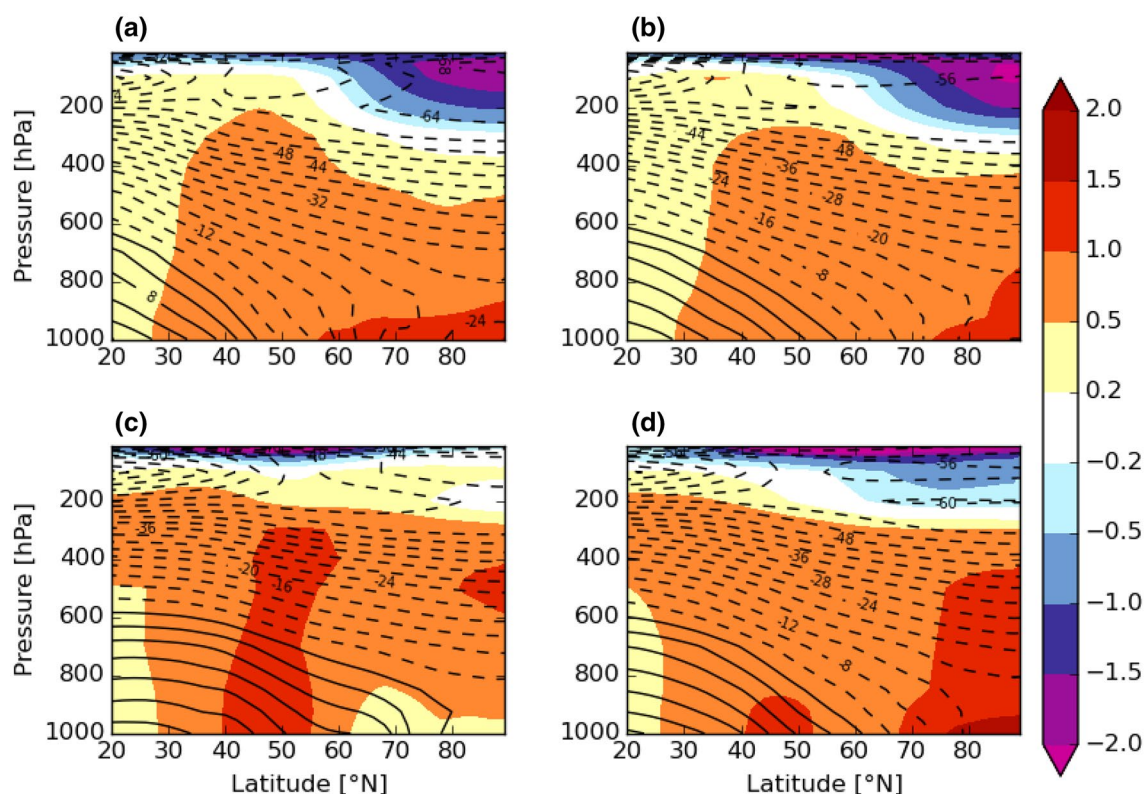


**Fig. 4** As in Fig. 3 but with  $1.65 \times \text{CO}_2$  concentration between 30 and 60° N (in the Northern mid-latitudes)

SICE simulations (not shown). These temperature anomalies are consistent with the geopotential height anomalies in 500 hPa (Fig. 8, up to around 50 m) indicating a barotropic response. The forcing excites a wave train with PNA (Pacific North America pattern) and EA (East Atlantic pattern) like anomalies. We also see a southward deflection of the jet stream in the eastern North Atlantic regions, redirecting the jet towards the Mediterranean Sea in the first 30 years after regionally quadrupling  $\text{CO}_2$  (Fig. 9).

In the second and third 30 year periods (Fig. 7b, c) some of the regional cold anomalies still persist (no warming over North Atlantic and slight cooling off the northeastern coast of Asia) but the large cold anomaly of up to around 1 °C over Central North America is replaced by a warm anomaly. Especially in the third 30 year period regional cold anomalies occur over other areas (Fig. 7c) but are not consistent across 60 N, 70 N, and SICE simulations and therefore not robust (not shown). Regional deviations from the zonal mean response are smaller in the second and third 30 year periods compared to the first 30 year period. In the last 60 years (Fig. 7d, e), apart from the strong warming over the Arctic that decreases with decreasing latitude within the northern mid-latitudes, a slight but rather homogeneous warming of around 0.2 °C prevails. Therefore, regional deviations from the zonal mean response in the last two 30 year periods are

smallest within the five 30 year periods. Similarly as for the 2 m temperature, for 500 hPa geopotential height and 300 hPa zonal wind regional anomalies become less robust over time (not shown). A reason for the weakening of the regional deviations from the zonal mean response over the simulation time, both in magnitude and robustness, could be that the ocean gradually warms; first adjacent to the Arctic forcing area and then the warming spreads out further, especially in the 60 N simulation. The slow adjustment of the ocean spreads out the initial temperature gradient weakening between Arctic and northern mid-latitudes to the south, making it again slightly stronger at the boundary of the forcing area. However, the meridional energy transport and the synoptic activity considered in the following two subsections do not show any trend towards a weakening response with simulation time.

Except for the temperature anomalies in the Arctic itself, temperature and circulation anomalies are rather small compared to the large intrinsic variability of the system, even in the first 30 years after quadrupling  $\text{CO}_2$  in the Arctic. Anomalies generally do not exceed 1 °C for the 2 m temperature, 50 m for Z500, and 5 m/s for the zonal wind in 300 hPa. One exception is the cold 2 m temperature anomaly over parts of North America related to the PNA-like anomaly in the first 30 years. Generally, our study prescribing greenhouse

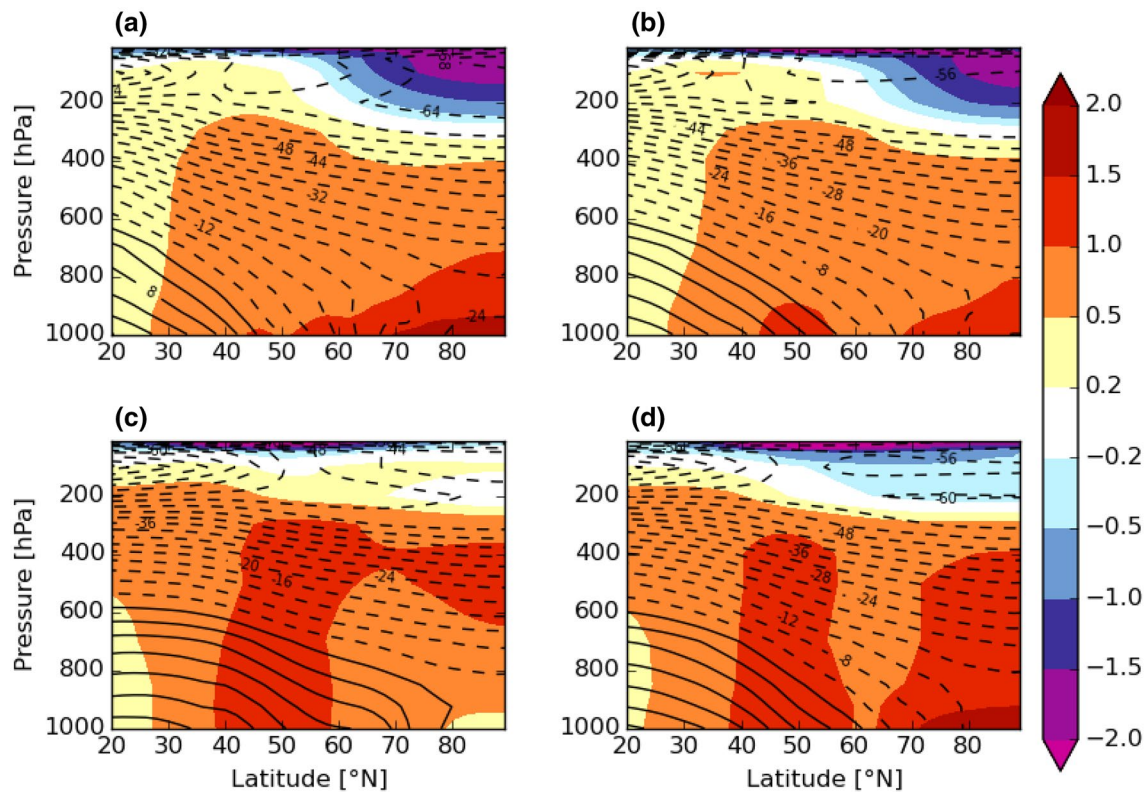


**Fig. 5** As in Fig. 3 but with  $4 \times \text{CO}_2$  concentration between 30 and  $60^\circ \text{N}$  (in the Northern mid-latitudes) scaled with the difference in forcing areas (area of Arctic divided by area of the Northern mid-latitudes)

gas forcing above and around the sea ice area confirms the weak response to Arctic sea ice anomalies that was found in previous studies.

### 3.3 Meridional energy transport

An analysis of the atmospheric meridional energy transport (Fig. 10a, c) reveals a decrease of the northward energy transport between around  $35^\circ \text{N}$  and  $80^\circ \text{N}$  in the Arctic forcing simulations 60 N, 70 N, and SICE compared to the control run. The decrease is most pronounced in the 60 N simulation (up to 0.13 PW). In other latitude belts differences are very small. This holds for both the first 30 years and also the following 120 years. The 30–60 N and 30–60 N\_1.65 simulations show increased northward energy transport north of around  $50^\circ \text{N}$  (up to 0.08 PW in 30–60 N simulation in the first 30 years) and a decreased northward energy transport south of around  $50^\circ \text{N}$  (up to 0.2 PW in 30–60 N simulation in the last 120 years) extending southward to about  $10^\circ$ – $50^\circ \text{S}$  depending on the considered time period and on the intensity of the forcing (30–60 N\_1.65 compared to 30–60 N). It is reassuring that qualitatively 30–60 N and 30–60 N\_1.65 simulations agree, i.e. scaling of the response with the magnitude of the forcing is justified.

The 60 Ns and glob simulations show large anomalies with respect to the control simulation across all latitudes which are due to the nearly global or global  $\text{CO}_2$  forcing. The anomalies generally work towards increased southward atmospheric energy transports in the Southern Hemisphere and towards increased atmospheric northward energy transports in the Northern Hemisphere, making the meridional energy transport towards the poles stronger almost everywhere. The response appears to be roughly additive, i.e. when adding the anomalies of the 60 N and the 60 Ns simulations (dashed orange lines in Fig. 10a, c), the result is similar to the anomalies of the glob simulation (solid orange lines in Fig. 10a, c); differences are smaller than 0.03 PW and are further decreasing over simulation time (compare Fig. 10a with Fig. 10c). This gives credibility to the regional forcing approach and is in agreement with Stuecker et al. (2018). However, the small differences between the sum of 60 N and 60 Ns simulations and the glob simulation are in the same direction across all latitudes north of  $40^\circ \text{S}$  and may therefore point to an important difference. The sum of 60 N and 60 Ns simulations shows a slightly stronger atmospheric northward energy transport across all latitudes north of  $40^\circ \text{S}$  than the glob simulation (compare dashed orange line in Fig. 10a with solid orange line). This can be attributed to the increased northward atmospheric energy transport in the

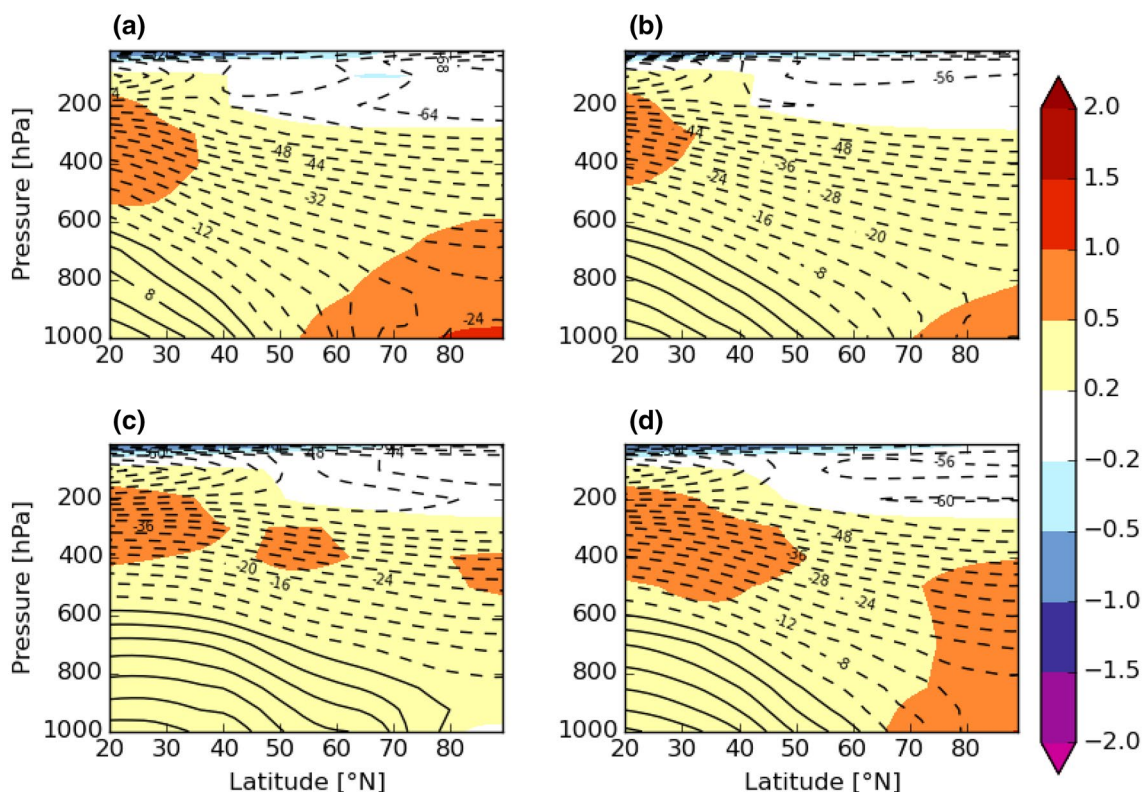


**Fig. 6** As in Fig. 3 but with  $4 \times \text{CO}_2$  concentration south of  $60^\circ \text{N}$  (extra-Arctic area) scaled with the difference in forcing areas (area of Arctic divided by area of extra-Arctic)

60 Ns simulation (brown line in Fig. 10a) compared to the glob simulation (solid orange line in Fig. 10a) which arises over all latitudes north of around  $40^\circ \text{S}$ . In contrast, when comparing the 60 N simulation to the control simulation (black curve in Fig. 10a)—which differs in the same way as the glob simulation from the 60 Ns simulation, namely by  $4 \times \text{CO}_2$  instead of  $1 \times \text{CO}_2$  in the Arctic—, anomalies in the northward atmospheric energy transport remain close to 0 south of around  $30^\circ \text{N}$ .

In the ocean (Fig. 10b, d) the situation is not as clear cut. Changes beyond the northern mid-latitudes occur also in the Arctic forcing simulations, for the larger forcing area (60 N) already in the first 30 and also in the following 120 years and for the weaker forcing areas (70 N and SICE) only in the following 120 years. Furthermore, no systematic difference can be seen between the sum of 60 N and 60 Ns simulations on one hand and the glob simulation on the other hand, at least not in the first 30 years. In the following 120 years there is a slight tendency towards stronger northward energy transport in the sum of 60 N and 60 Ns simulations compared to the glob simulation. Anomalies in the global and nearly global forcing experiments glob and 60 Ns generally work towards a weaker poleward oceanic energy transport which is in contrast to the atmospheric transport. While in the ocean anomalies clearly grow over time for all simulations—around  $20^\circ$

S by as much as 0.25 PW in the global and nearly global forcing experiments when comparing the last 120 years to the first 30 years—in the atmosphere they grow only slightly by less than 0.05 PW or they remain constant.

### 3.4 Synoptic activity

The reduced atmospheric northward energy transport in the Arctic forcing experiments is also reflected by a slightly reduced synoptic activity in the northern mid-latitudes (Fig. 11a for the 60 N experiment in boreal winter (DJF), also true for 70 N and SICE experiments and for the other seasons) due to reduced meridional temperature gradients in these experiments which can cause less energy exchange. An exception is the area over the Greenland, Norwegian, Iceland (GIN) Seas in DJF (Fig. 11a) and the Arctic north of  $80^\circ \text{N}$  in JJA (not shown) where the synoptic activity increases by up to 2–3 m—which is very little compared to the variability in these areas.

Similarly, the increased atmospheric northward energy transport north of  $50^\circ \text{N}$  in the mid-latitude forcing experiments is generally reflected by an increased synoptic activity in these latitudes, especially over the GIN seas, and the decreased energy transport south of  $50^\circ \text{N}$  by a decreased

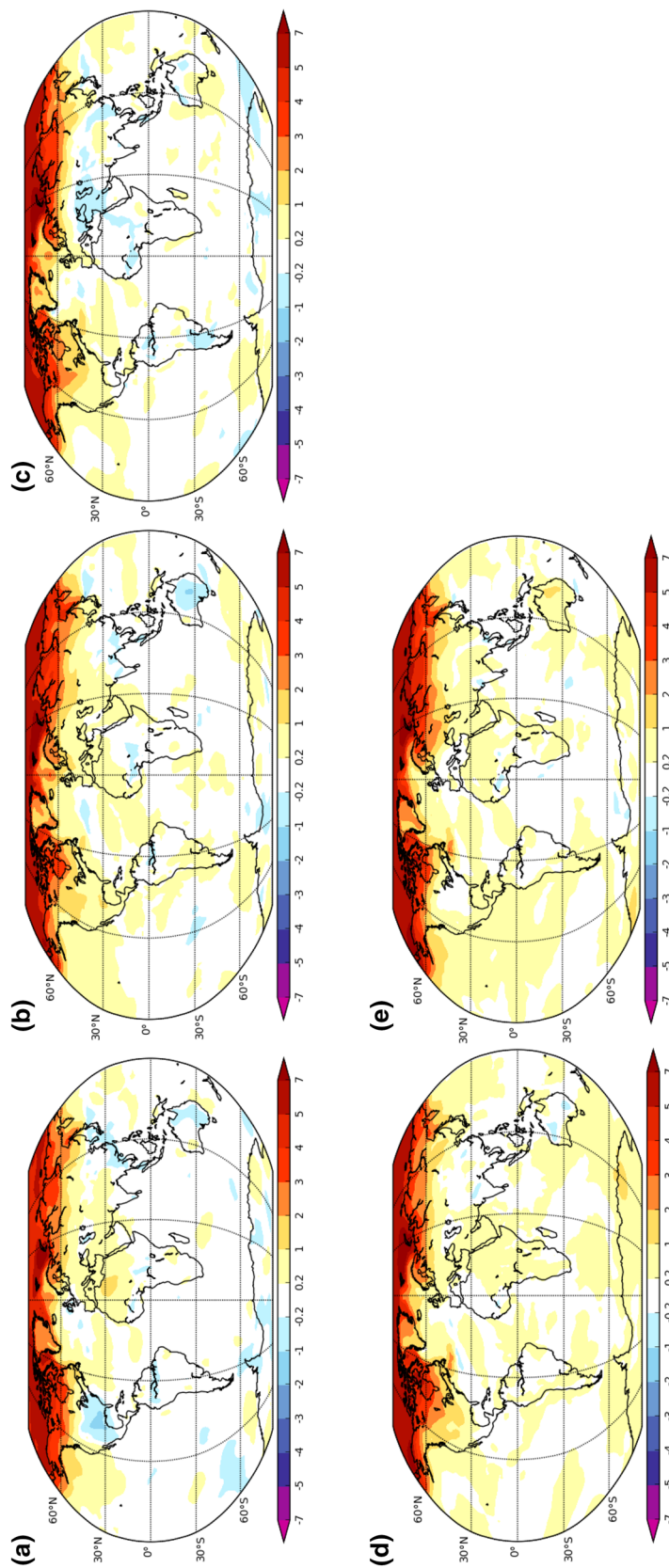


**Fig. 7** Response in DJF 2 m temperature (K) in 60 N simulation, averaged over the first 30 years after regionally quadrupling CO<sub>2</sub>, **b** averaged over the second 30 years, **c** averaged over the third 30 years, **d** averaged over the fourth 30 years, and **e** averaged over the last 30 years

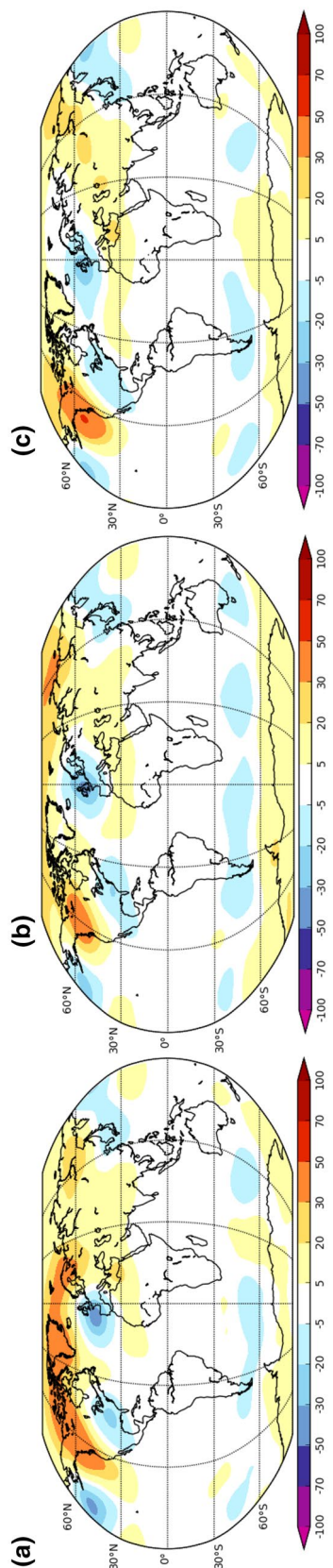


**Fig. 8** Response in DJF 500 hPa geopotential height (m) in **a** 60 N simulation, **b** 70 N simulation, and **c** SICE simulation averaged over the first 30 years after regionally quadrupling CO<sub>2</sub>

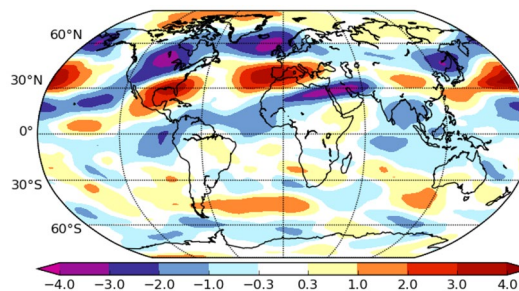


**Fig. 9** Response in DJF 300 hPa u component (m/s) in 60 N simulation averaged over the first 30 years after regionally quadrupling CO<sub>2</sub>

synoptic activity (Fig. 11b, c for DJF, also true for the other seasons).

In the 60 Ns and glob experiments there are areas of strengthened and weakened synoptic activity (not shown). Especially in the Southern Hemisphere the poleward shift of intense synoptic activity typical for greenhouse gas increase experiments (e.g. Tamarin and Kaspi 2017) becomes obvious. In the Northern Hemisphere no poleward shift occurs. Instead, an intensification of synoptic activity along the jet stream path over the North Pacific and an eastward extension over the North Atlantic into Europe is simulated. In summary, in the 30–60 N, 30–60 N\_1.65, 60 Ns and glob experiments synoptic activity is redistributed while in the Arctic forcing experiments it is reduced with the reduction being confined to the area of meridional temperature gradient reduction.

The weak linkage between the mid-latitudes and the Arctic in the Arctic forcing simulations is reflected by a large decrease of Arctic sea ice volume (Fig. 1 black and grey lines, around 12,000 km<sup>3</sup> in 60 N compared to control)—an indication that the extra energy stays in the Arctic and causes melting of the sea ice. The same Arctic sea ice volume decrease is simulated when 4\* CO<sub>2</sub> is applied in the northern mid-latitudes 30–60° N (Fig. 1, purple line). Obviously, when the magnitude of the global radiative forcing is considered to make the northern mid-latitude forcing simulation comparable to the Arctic forcing simulation, the Arctic sea ice volume decrease is weaker (Fig. 1, green line).

## 4 Discussion and conclusions

In this study, a novel approach is used to explore the impact of Arctic climate change on mid-latitudes and vice versa in a coupled climate model. In this approach, which recently has been also employed by Stuecker et al. (2018), atmospheric CO<sub>2</sub> concentrations are quadrupled in certain regions, while keeping other regions unchanged. An important result of this study, which is consistent with previous work, is that

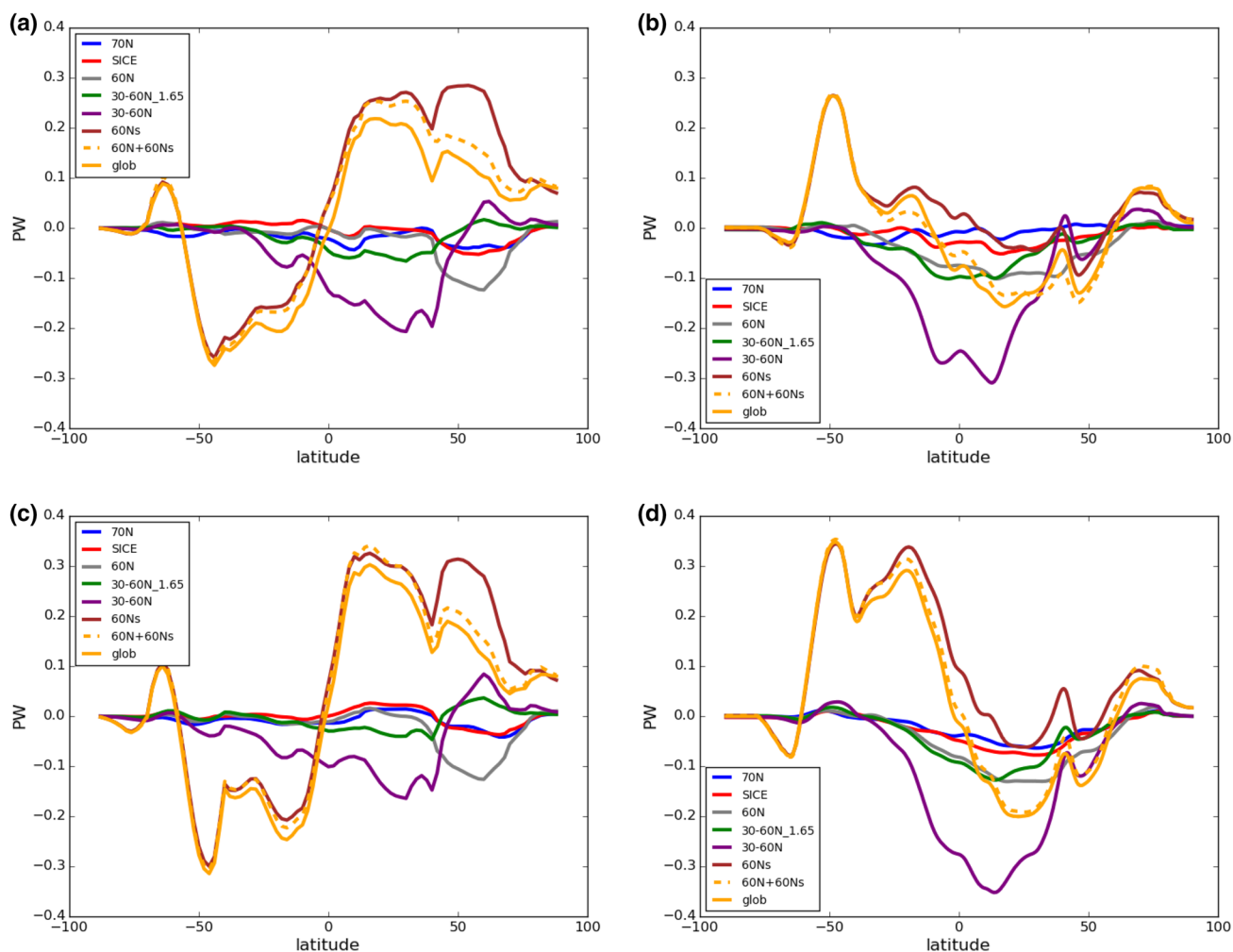


**Fig. 10** Northward **a** atmospheric and **b** oceanic energy transport response (PW) averaged over the first 30 years. **c, d** As **a** and **b** but for the last 120 years. The orange dashed line shows the sum of the anomalies from the 60 N and the 60 Ns simulation. The non-zero

energy transport at 90° N is due to the uptake of heat from the ocean and indicates that the ocean is not in equilibrium, especially in 60 Ns and glob simulations

the Arctic generally shows a relatively limited influence on extra-Arctic regions, while CO<sub>2</sub> changes in the extra-Arctic region lead to substantial changes in the Arctic. The energy added in the regional Arctic forcing experiments stays in the Arctic causing efficient reduction of the Arctic sea ice; the synoptic activity is reduced, weakening the link between Arctic and mid-latitudes. Nevertheless, there are some important insights to be gained from the regional Arctic forcing experiments which are described in the following before turning to the extra-Arctic forcing.

When Arctic sea ice is reduced because of the CO<sub>2</sub> forcing, the vertical temperature profile in the atmosphere changes in the Arctic. In the Arctic troposphere, the changes are consistent with those found in previous studies reducing Arctic sea ice, i.e. most of the warming takes place close to the surface. However, in the Arctic stratosphere cooling is simulated. Our simulations, thus, suggest that there is a

stronger stratospheric polar vortex in late winter in contrast to a weaker one like some previous studies investigating the response to reduced Arctic sea ice reported (e.g. Jaiser et al. 2013; Kim et al. 2014)—although the stratospheric response is sensitive to the location of Arctic sea ice loss (e.g. Sun et al. 2015). The strengthened stratospheric polar vortex in our Arctic forcing experiments needs to be taken into consideration when interpreting the results presented here. Even though it has been observed that the intensity of the stratospheric polar vortex has decreased in recent decades (e.g. Kretschmer et al. 2018), it is not clear if this is due to Arctic sea ice decline or due to other factors. Also unclear is how the stratospheric polar vortex will develop in a warming climate (Ayarzagüena et al. 2018).

In our study, we use a different model than Stuecker et al. (2018) (AWI-CM 1.1 instead of CESM2) and consider different regions (more focus on the Arctic region with three

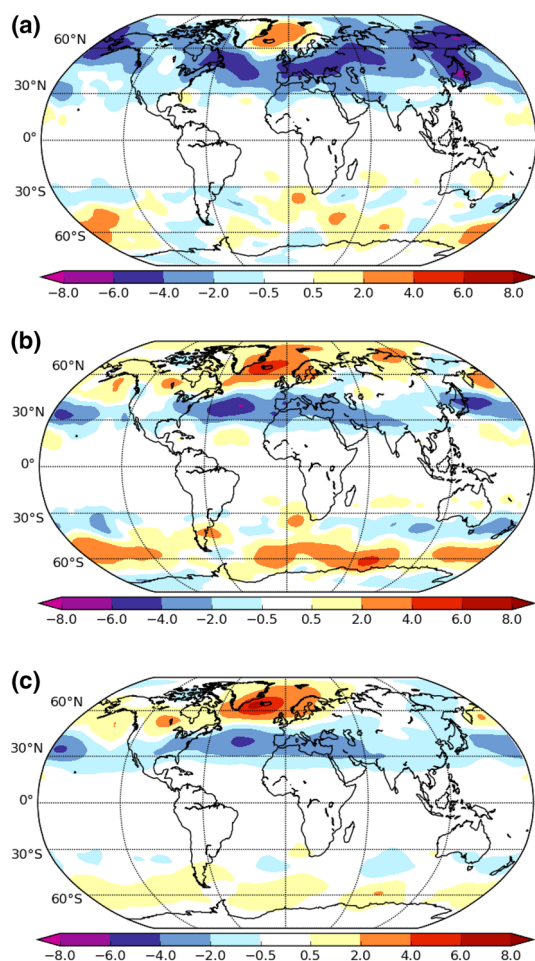


**Fig. 11** Response in DJF synoptic activity in 500 hPa (m) for the last 120 years **a** for 60 N, **b** for 30–60 N<sub>1.65</sub>, and **c** for 30–60 N scaled with the forcing areas

different set-ups as well as the northern mid-latitudes with two different set-ups while leaving the Southern Hemisphere untouched). Furthermore, we also consider longer time scales, which gives us an insight into the transient versus the quasi-equilibrium response; and additional analyses are carried out that address large-scale circulation changes including synoptic activity.

An important result is that only in the adjustment phase in the first 30 years after adding the perturbation, there are robust regional near-surface temperature and large-scale circulation changes such as surface cooling of more than 1 °C over parts of North America and up to around 0.2 °C over eastern Asia in winter. The pattern of strongest warming over the Barents-Kara Seas and the East Siberian and-Chukchi Sea areas along with cold anomalies over North America and over eastern Asia are reminiscent of the observed temperature trend pattern of the last two decades (e.g. Kug et al. 2015) although in our simulations the East Siberian and-Chukchi Sea warming is extended into the Beaufort

Sea, and the cold anomaly is restricted to the very eastern parts of Asia. The latter pattern could be caused by the fact that we do not have a weakening but a strengthening of the stratospheric polar vortex. Therefore, weak stratospheric vortex events are less likely in our Arctic forcing experiments. However, more weak stratospheric vortex events have occurred in the recent two decades. Through downward propagation this can cause northern Eurasia cold events. Indeed this had led to a cooling trend even in the average in some Northern Eurasian areas (e.g. Kretschmer et al. 2018). The strengthening of the stratospheric polar vortex along with the advection of less cold air in cases of northerly flow could lead to the relatively strong warming trend over northern Eurasia in our Arctic forcing experiments.

After the first 30 years, the magnitude of the anomalies decreases. This is an important result given that the most rapid Arctic changes were observed in the last 30 years. Because of this similarity between observations and model simulations, one might speculate if once a hiatus in Arctic amplification occurs for example due to natural variability, the expected circulation and temperature anomalies would decrease in intensity or even disappear. However, our experiments are highly idealized and our experiments consider a sudden rather than transient forcing which then leads to transient changes.

A plausible explanation of the behavior in the simulations could be that the initial warming occurring in the Arctic due to the regional CO<sub>2</sub> forcing spreads out slowly into lower latitudes due to the long ocean adjustment time scale. In this respect our results agree with the coupled Arctic sea ice reduction experiments described in Screen et al. (2018). Therefore, the initial differential heating is not restricted to the Arctic anymore. The initial marked meridional temperature gradient reduction around 60° N is getting spread out towards lower latitudes. However, the meridional energy transport and the synoptic activity response do not show any trend towards a weaker response with simulation time.

It has also been discussed if a weaker meridional temperature gradient may cause more extreme events due to a weakened jet stream and amplified and slower moving planetary waves. However, given the shallowness of the Arctic temperature increase and the strong natural variability it is difficult to get a robust response (Vavrus 2018). When we look at the variability on time scales beyond the synoptic scale in our three Arctic forcing simulations we see a robust, up to around 0.5 °C higher 2-m winter temperature variability over Siberia in the first 30 years. In other regions there is no consistent pattern. Averaged over the northern mid-latitudes there is not much change. After the first 30 years there is a decrease in 2 m winter temperature variability in most northern mid-latitude areas.

While there are some consistent but weak mid-latitude features in the transient response to the regional Arctic

forcing, the influence of extra-Arctic forcing on the Arctic is clearly more important. Efficient Arctic sea ice reduction can occur in absence of Arctic CO<sub>2</sub> forcing by quadrupling CO<sub>2</sub> only south of 60° N (extra-Arctic forcing) or in the northern mid-latitudes between 30 and 60° N. While the temperature close to the surface strongly increases north of the forcing area 30–60° N, this does not happen south of the forcing area. This is also true when the forcing in 30–60° N is reduced to 1.65 × CO<sub>2</sub> in order to consider the larger forcing area compared to the area of north of 60° N. Due to an increased northward atmospheric energy transport and increased high-latitude synoptic activity in the extra-Arctic and northern mid-latitude forcing simulations, Arctic sea ice reduction is triggered, and consequently Arctic Amplification occurs, despite the lack of Arctic CO<sub>2</sub> forcing. In the extra-Arctic and global forcing experiments an increased high-latitude northward oceanic energy transport of up to 0.1 PW occurs. This could also contribute to Arctic sea ice decline and Arctic Amplification; the slow component of Arctic sea ice decline in Fig. 1 in these simulations supports this notion. In the Arctic forcing experiments decreased northward atmospheric energy transport compared to the control simulation is only present in the northern high- and mid-latitudes. Therefore, the Arctic forcing only impacts the mid-latitudes in the atmosphere. However, in the ocean the Arctic forcing does play a role also for the low latitude northward energy transport which is decreased compared to the control simulation at least after the initial 30 years by up to 0.12 PW.

While the atmospheric energy transport is generally larger in magnitude than the oceanic energy transport by a factor of around 3 in northern high-latitudes in all experiments, the anomalies between sensitivity experiments on one hand and the control experiment on the other hand are of comparable magnitude (see Fig. 10). This indicates that the ocean plays an important role in redistributing the energy in the sensitivity experiments. For the northern mid-latitude forcing experiments, the ocean even plays a larger role in the redistribution of the extra energy compared to the atmosphere. Anomalies in low latitude northward energy transport amount to up to -0.35 PW in the ocean and only up to -0.2 PW in the atmosphere.

In the first 15 years of the 60 Ns simulation around half of the Arctic sea ice volume is gone due to the CO<sub>2</sub> forcing south of 60° N (Fig. 1). In the remaining 135 years of the simulation another sixth of the original Arctic sea ice volume disappears bringing the total reduction to two thirds. The fast adjustment in the first 15 years versus the slower adjustment in the remaining simulation time indicates that the atmospheric contribution to the sea ice melt decreases over time.

We propose that the method of regionally increased CO<sub>2</sub> concentrations should be used in a set of coordinated

experiments with as many different climate models as possible. The PAMIP community could decide to take such experiments onboard as additional experiments since it has been shown by both Stuecker et al. (2018) and in this study that the method works to decompose the regional impacts of CO<sub>2</sub> concentrations. However, there are important differences in the results between the two studies. In our study the meridional oceanic and atmospheric energy transport plays a major role for Arctic amplification while Stuecker et al. (2018) point to the local processes as a major source of Arctic amplification. In our study the response in the meridional atmospheric energy transport to the regional forcing is additive in the polar regions while in the low latitudes an increased northward energy transport is simulated for the sum of extra-Arctic forcing and Arctic forcing compared to the global forcing.

It is not clear if the differences between the two studies are due to the different model formulations or due to the different experiment set-up (in the case of Stuecker et al. 2018, the forcing is symmetric between the two hemispheres; in our case the set-up is asymmetric). Therefore the call for coordinated experiments. Causes and impacts of Arctic amplification could be studied in an idealized and consistent way, and the robustness of the results could be checked by comparing multiple climate models.

**Acknowledgements** Open Access funding provided by Projekt DEAL. We are grateful to the DKRZ (German computing center) for providing us with computing time. This work has been carried out within the project APPLICATE which has received funding from the European Union's Horizon 2020 research and innovation programme under Grant agreement No. 727826. We thank Claudia Hinrichs for critical reading of our manuscript and her constructive comments. Furthermore we thank the anonymous reviewer for constructive comments and suggestions.

**Open Access** This article is licensed under a Creative Commons Attribution 4.0 International License, which permits use, sharing, adaptation, distribution and reproduction in any medium or format, as long as you give appropriate credit to the original author(s) and the source, provide a link to the Creative Commons licence, and indicate if changes were made. The images or other third party material in this article are included in the article's Creative Commons licence, unless indicated otherwise in a credit line to the material. If material is not included in the article's Creative Commons licence and your intended use is not permitted by statutory regulation or exceeds the permitted use, you will need to obtain permission directly from the copyright holder. To view a copy of this licence, visit <http://creativecommons.org/licenses/by/4.0/>.

## References

- Ayarzagüena B, Screen JA (2016) Future Arctic sea ice loss reduces severity of cold air outbreaks in mid-latitudes. *Geophys Res Lett* 43:2801–2809. <https://doi.org/10.1002/2016GL068092>
- Ayarzagüena B, Polvani LM, Langematz U, Akiyoshi H, Bekki S, Butchart N, Dameris M, Deushi M, Hardiman SC, Jöckel P,

- Klekociuk A, Marchand M, Michou M, Morgenstern O, O'Connor FM, Oman LD, Plummer DA, Revell L, Rozanov E, Saint-Martin D, Scinocca J, Stenke A, Stone K, Yamashita Y, Yoshida K, Zeng G (2018) No robust evidence of future changes in major stratospheric sudden warmings: a multi-model assessment from CCMI. *Atmos Chem Phys* 18:11277–11287. <https://doi.org/10.5194/acp-18-11277-2018>
- Cohen J, Screen JA, Furtado JC, Barlow M, Whittleston D, Coumou D, Francis J, Dethloff K, Entekhabi D, Overland J, Jones J (2014) Recent Arctic amplification and extreme mid-latitude weather. *Nat Geosci* 7:627–637. <https://doi.org/10.1038/ngeo2234>
- Cohen J, Zhang X, Francis J, Jung T, Kwok R, Overland J, Taylor PC, Lee S, Laliberté F, Feldstein S, Maslowski W, Henderson G, Stroeve J, Coumou D, Handorf D, Semmler T, Ballinger T, Hell M, Kretschmer M, Vavrus S, Wang M, Wang S, Wu Y, Vihma T, Bhatt U, Ionita M, Linderholm H, Rigor I, Rouston C, Singh D, Wendisch M, Smith D, Screen J, Yoon J, Peings Y, Chen H, Blackport R (2018) Arctic change and possible influence on mid-latitude climate and weather. US CLIVAR Report 2018-1, 41pp. <https://doi.org/10.5065/D6TH8KGW>
- Garfinkel C, Son S-W, Song K, Aquila V, Oman LD (2017) Stratospheric variability contributed to and sustained the recent hiatus in Eurasian winter warming. *Geophys Res Lett* 44:374–382. <https://doi.org/10.1002/2016GL072035>
- Gong T, Feldstein S, Lee S (2017) The role of downward infrared radiation in the recent Arctic winter warming trend. *J Clim* 30:4937–4949. <https://doi.org/10.1175/JCLI-D-16-0180.1>
- Gregory JM, Ingram WJ, Palmer MA, Jones GS, Stott PA, Thorpe RB, Lowe JA, Johns TC, Williams KD (2004) A new method for diagnosing radiative forcing and climate sensitivity. *Geophys Res Lett* 31:L03205. <https://doi.org/10.1029/2003GL018747>
- Haarsma RJ, Roberts MJ, Vidale PL, Senior CA, Bellucci A, Bao Q, Chang P, Corti S, Fuckar NS, Guemas V, von Hardenberg J, Hazeleger W, Kodama C, Koenigk T, Leung LR, Lu J, Luo J-J, Mao J, Mizielinski MS, Mizuta R, Nobre P, Satoh M, Scoccimarro E, Semmler T, Small J, von Storch J-S (2016) High Resolution Model Intercomparison Project (HighResMIP v1.0) for CMIP6. *Geosci Model Dev* 9:4185–4208. <https://doi.org/10.5194/gmd-9-4185-2016>
- Jaiser R, Dethloff K, Handorf D (2013) Stratospheric response to Arctic sea ice retreat and associated planetary wave propagation changes. *Tellus A* 65:19375. <https://doi.org/10.3402/tellusa.v65i0.19375>
- Kim B-M, Son S-W, Min S-K, Jeong J-H, Kim S-J, Zhang X, Shim T, Yoon J-H (2014) Weakening of the stratospheric polar vortex by Arctic sea-ice loss. *Nat Commun* 5:4646. <https://doi.org/10.1038/ncomms5646>
- Kug J-S, Jeong J-H, Jang Y-S, Kim B-M, Folland C-K, Min S-K, Son S-W (2015) Two distinct influences of Arctic warming on cold winters over North America and East Asia. *Nat Geosci*. <https://doi.org/10.1038/NNGEO2517>
- Luo B, Wu L, Luo D, Dai A, Simmonds I (2018) The winter midlatitude-Arctic interaction: effects of North Atlantic SST and high-latitude blocking on Arctic sea ice and Eurasian cooling. *Clim Dyn*. <https://doi.org/10.1007/s00382-018-4301-5>
- Overland J, Francis JA, Hall R, Hanna E, Kim S-J, Vihma T (2015) The melting Arctic and midlatitude weather patterns: are they connected? *J Clim* 28:7917–7932. <https://doi.org/10.1175/JCLI-D-14-00822.1>
- Overland JE, Dethloff K, Francis JA, Hall RJ, Hanna E, Kim S-J, Screen JA, Shepherd TG, Vihma T (2016) Nonlinear response of mid-latitude weather to the changing Arctic. *Nat Clim Change* 6:992–999. <https://doi.org/10.1038/NCLIMATE3121>
- Pedersen RA, Cvijanovic C, Langen PL, Vinther BM (2016) The impact of regional Arctic sea ice loss on atmospheric circulation and the NAO. *J Clim* 29:889–902. <https://doi.org/10.1175/JCLI-D-15-0315.1>
- Petrie RE, Shaffrey LC, Sutton RT (2015) Atmospheric impact of Arctic sea ice loss in a coupled ocean-atmosphere simulation. *J Clim* 28:9606–9622. <https://doi.org/10.1175/JCLI-D-15-0316.1>
- Pithan F, Mauritsen T (2014) Arctic amplification dominated by temperature feedbacks in contemporary climate models. *Nat Geosci* 7:181–184. <https://doi.org/10.1038/NNGEO2071>
- Rackow T, Goessling HF, Jung T, Sidorenko D, Semmler T, Barbi D, Handorf D (2018) Towards multi-resolution global climate modeling with ECHAM6-FESOM. Part II: climate variability. *Clim Dyn* 50:2369–2394. <https://doi.org/10.1007/s00382-016-3192-6>
- Rackow T, Sein D, Semmler T, Danilov S, Koldunov N, Sidorenko D, Wang Q, Jung T (2019) Sensitivity of deep ocean biases to horizontal resolution in prototype CMIP6 simulations with AWI-CM 1.0. *Geosci Model Dev Discuss*. <https://doi.org/10.5194/gmd-2018-192>
- Screen JA, Simmonds I, Deser C, Tomas R (2013) The atmospheric response to three decades of observed Arctic sea ice loss. *J Clim* 26:1230–1248. <https://doi.org/10.1175/JCLI-D-12-00063.1>
- Screen JA, Deser C, Smith DM, Zhang X, Blackport R, Kushner PJ, Oudar T, McCusker KE, Sun L (2018) Consistency and discrepancy in the atmospheric response to Arctic sea-ice loss across climate models. *Nat Geosci* 11:155–163. <https://doi.org/10.1038/s41561-018-0059-y>
- Semmler T, McGrath R, Wang S (2012) The impact of Arctic sea ice on the Arctic energy budget and on the climate of the Northern mid-latitudes. *Clim Dyn* 39:2675–2694. <https://doi.org/10.1007/s00382-012-1353-9>
- Semmler T, Jung T, Serrar S (2016a) Fast atmospheric response to a sudden thinning of Arctic sea ice. *Clim Dyn* 46:1015–1025. <https://doi.org/10.1007/s00382-015-2629-7>
- Semmler T, Stulic L, Jung T, Tilinina N, Campos C, Gulev S, Koracin D (2016b) Seasonal atmospheric responses to reduced Arctic sea ice in an ensemble of coupled model simulations. *J Clim* 29:5893–5913. <https://doi.org/10.1175/JCLI-D-15-0586.1>
- Seviour WJM (2017) Weakening and shift of the Arctic stratospheric polar vortex: internal variability or forced response? *Geophys Res Lett* 44:3365–3373. <https://doi.org/10.1002/2017GL073071>
- Sidorenko D, Rackow T, Jung T, Semmler T, Barbi D, Danilov S, Dethloff K, Dorn W, Fieg K, Goessling HF, Handorf D, Harig S, Hiller W, Juricke S, Losch M, Schröter J, Sein DV, Wang Q (2015) Towards multi-resolution global climate modeling with ECHAM6-FESOM. Part I: model formulation and mean climate. *Clim Dyn* 44:757–780. <https://doi.org/10.1007/s00382-014-2290-6>
- Smith DM, Screen JA, Deser C, Cohen J, Fyfe JC, Garcia-Serrano J, Jung T, Kattsov V, Matei D, Msadek R, Peings Y, Sigmund M, Ukita J, Yoon J-H, Zhang X (2018) The Polar Amplification Model Intercomparison Project (PAMIP) contribution to CMIP6: investigating the causes and consequences of polar amplification. *Geosci Model Dev Discuss*. <https://doi.org/10.5194/gmd-2018-82>
- Stuecker MF, Bitz CM, Armour KC, Proistosescu C, Kang SM, Xie S-P, Kim D, McGregor S, Zhang W, Zhao S, Cai W, Dong Y, Jin F-F (2018) Polar amplification dominated by local forcing and feedbacks. *Nat Clim Change*. <https://doi.org/10.1038/s41558-018-0339-y>
- Sun L, Deser C, Tomas RA (2015) Mechanisms of stratospheric and tropospheric circulation response to projected Arctic Sea ice loss. *J Clim* 28:7824–7845. <https://doi.org/10.1175/JCLI-D-15-0169.1>
- Tamarin T, Kaspi Y (2017) The poleward shift of storm tracks under global warming: a Lagrangian perspective. *Geophys Res Lett*. <https://doi.org/10.1002/2017GL073633>
- Vavrus SJ (2018) The influence of Arctic Amplification on Mid-latitude Weather and Climate. *Curr Clim Change Rep* 4:238–249. <https://doi.org/10.1007/s40641-018-0105-2>

- Woods C, Caballero R (2016) The role of moist intrusions in winter Arctic warming and sea ice decline. *J Clim* 29:4473–4485. <https://doi.org/10.1175/JCLI-D-15-0773.1>
- Zappa G, Pithan F, Shepherd G (2018) Multimodel evidence for an atmospheric circulation response to Arctic sea ice loss in the CMIP5 future projections. *Geophys Res Lett* 45:1011–1019. <https://doi.org/10.1002/2017GL076096>

**Publisher's Note** Springer Nature remains neutral with regard to jurisdictional claims in published maps and institutional affiliations.